Self-supported MOF/Cellulose-nanocrystals materials designed from ultrafiltration

Lorenzo Metilli[1], Héloïse Ugo[2], William Chèvremont[3], Cyril Picard[2] and Frédéric Pignon[1]

[1]*Univ. Grenoble Alpes, CNRS, Grenoble INP (Institute of Engineering Univ. Grenoble Alpes), LRP, 38000 Grenoble, France*
[2]*Univ. Grenoble Alpes, CNRS, LIPhy (Laboratoire Interdisciplinaire de Physique), Université Grenoble Alpes, 38000 Grenoble, France*
[3]*ESRF, The European Synchrotron, 38043 Grenoble, France*

lorenzo.metilli@univ-grenoble-alpes.fr

Supporting Information

The CNC suspensions were prepared by mixing and sonication, transferred into quartz capillaries and analysed at ESRF beamline TRUSAXS with a sample-detector distance (SDD) of 1.5 and 10 metres. The azimuthally-averaged scattering intensity of a diluted sample (0.14 wt. %) was fitted with a parallelepiped model, using the software Sasview (Figure S1a). Due to the limited q-range available, it was not possible to determine the length of the CNC; the value was therefore set to 120 nm, which was the average length measured from the TEM images of the samples. The width and height of the CNC was estimated to be 3.4 nm and 16.2 nm, respectively.

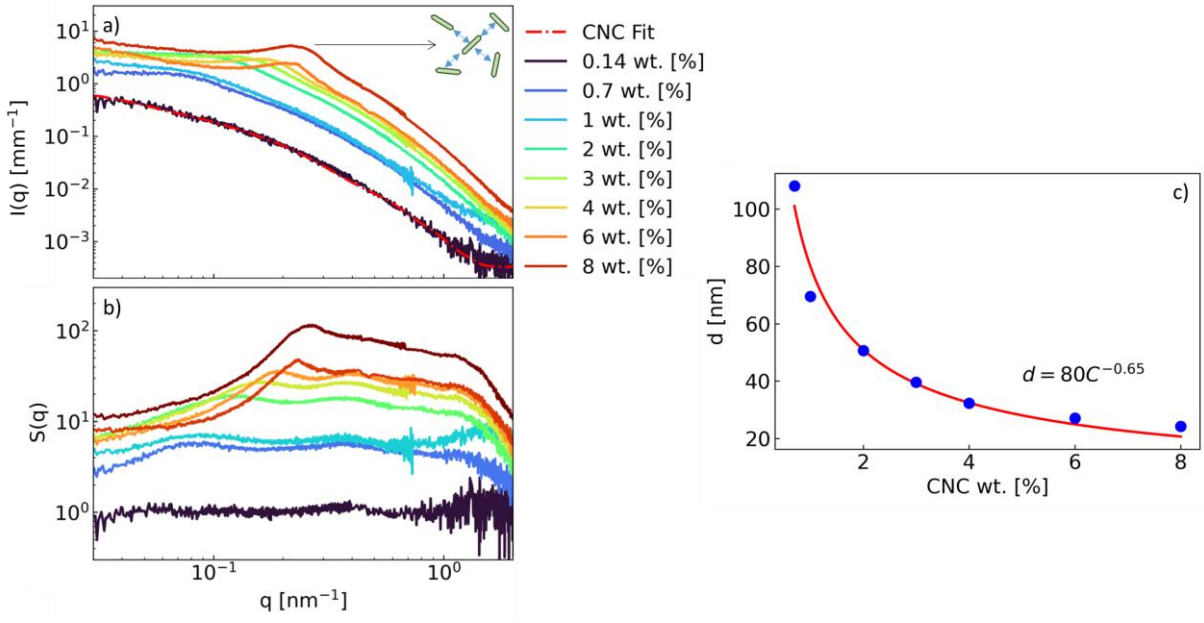

Figure S1. (a) Azimuthally-averaged scattering intensity of CNC suspensions at different weight concentrations, (b) corresponding structure factors obtained by dividing by the form factor F(q) and c) interparticle distance peak as a function of concentration, fitted by a single-decay exponential.

The colloidal stability of ZIF-8 suspension with and without CNC was investigated macroscopically by pouring 20 mL of the suspensions in glass test tubes, and observing its evolution over time (Figure S2).

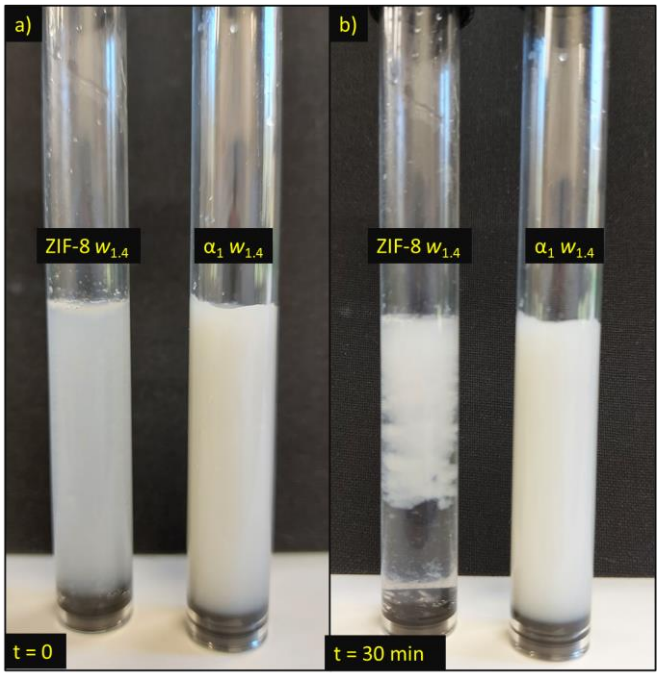

Figure S2. Photographs showing the stability to phase separation (creaming, in this case) of an aqueous ZIF-8 suspension at 1.4 mass fraction, compared to an $\alpha_1 w_{1.4}$ suspension (1:1 CNC:ZIF-8 volume ratio) after 30 minutes from mixing. When not mixed with CNCs, the ZIF-8 particles start aggregating, flocculating to visible, millimetric aggregates, eventually rising to the surface of the suspension. Instead, after addition and sonication of CNCs, the suspension remains homogeneous.

The crystalline nature of ZIF-8 was assessed using Wide Angle X-Ray Scattering (WAXS) at TRUSAXS (ESRF, Grenoble). The scattering patter was compared with the one reported by Almasoudi & Mokaya, (2012), which represents the same ZIF-8 product (Basolite Z1200®)

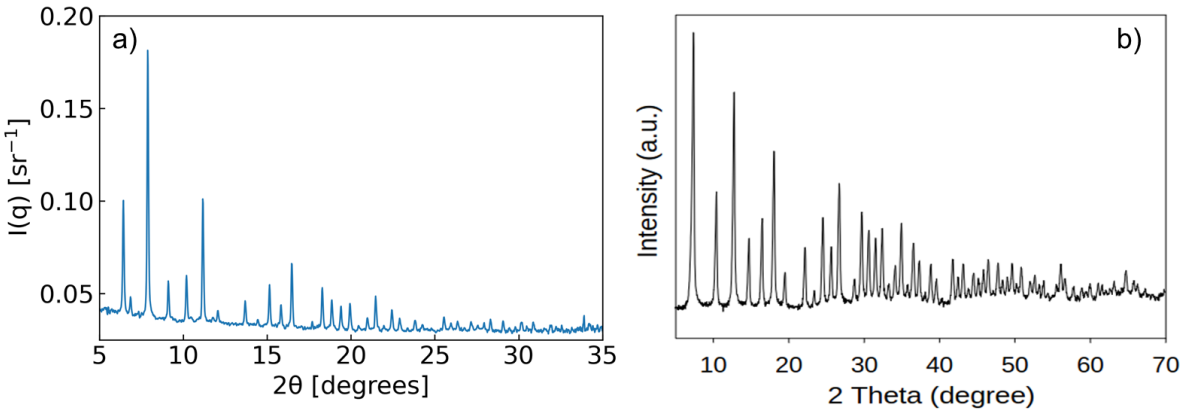

Figure S3. WAXS pattern of Basolite Z1200® ZIF-8 powder used in this work (a) compared with the one reported in literature by Almasoudi & Mokaya (2012) (b), adapted with from Almasoudi & Mokaya (2012) with permission from the Royal Society of Chemistry.

The sonication of ZIF-8 particles was carried out using a 100% duty cycle, maximum power level. The particle size distribution was measured with laser diffraction every 60 seconds (Figure S4).

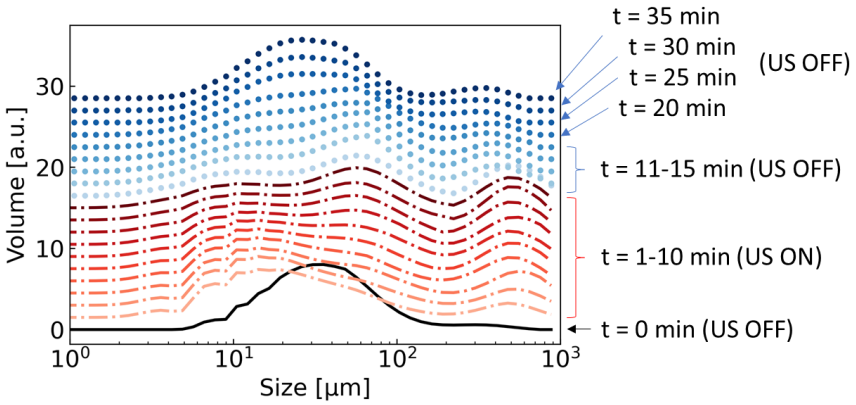

Figure S4. Particle size distribution of a ZIF-8 aqueous suspension during sonication, measured by laser scattering. The black curve is the suspension at rest (t=0), red curves are measured while sonicating (t = 1-10 min) and the dotted blue curves are measured during relaxation (t = 11 – 35 min). Volume % are shifted on the y axis for clarity.

The TEM images of CNCs were analysed using ImageJ 1.52t, using the "measure" function (Figure S5), in order to obtain an estimate of the size of CNCs.

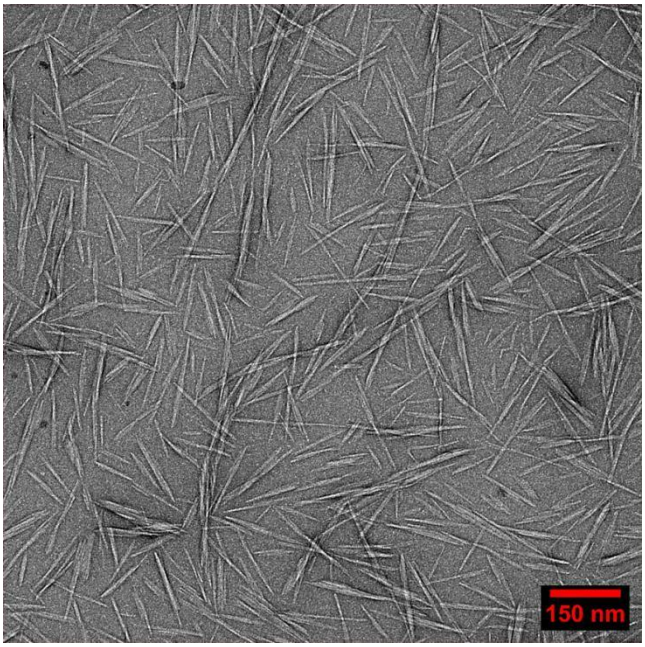

Figure S5. TEM image of an aqueous suspension of sonicated CNCs.

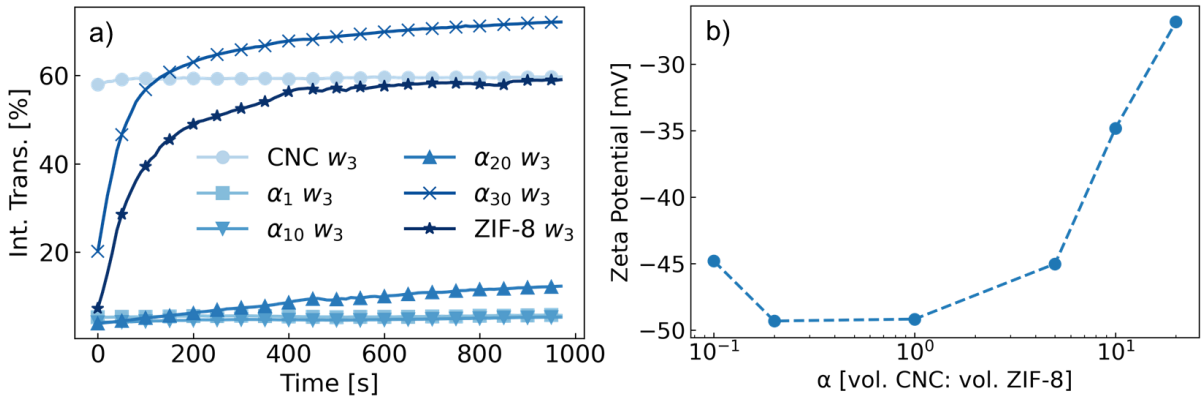

Figure S6. a) Evolution of the light transmission during centrifugation at 250 rpm and (b) zeta potential of samples with different α values.

The particle size measurements, obtained by static light scattering, showed that the physical mixing of CNC with ZIF-8 was not effective in decreasing the mean ZIF-8 aggregate size. On the other hand, the sonication process allowed the reduction of the particles' aggregate size from *ca.* 40 µm to 20 µm. Furthermore, within the explored α values range, the quantity of CNCs did not affect the final size distribution of the ZIF-8 aggregates during sonication (Figure S7b).

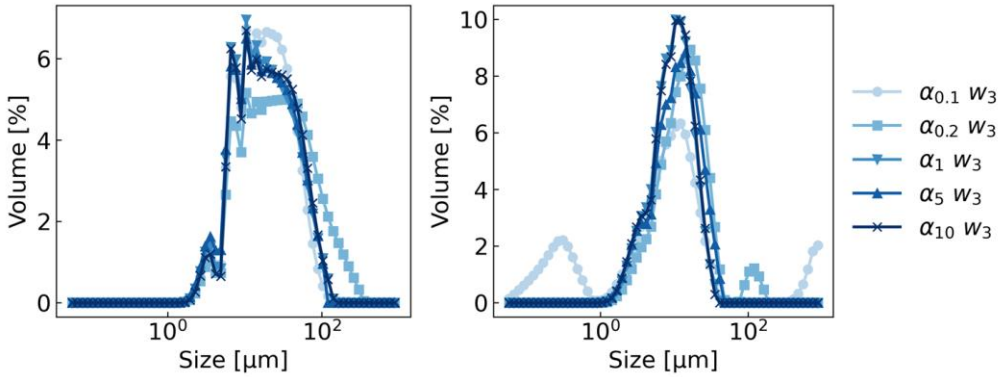

Figure S7. Size distribution of ZIF-8:CNC aggregates, measured by static light scattering, with different α values, after mixing for 1 hour (a) and after sonication for 15 minutes (b).

The rheological data collected during shear flow experiments of samples with different α values (see Table S1) were fitted using the Power Law model; the data from ZIF-8 suspension, instead, was fitted using the Herschel-Bulkley model. The results are shown in Figure S8.

Table S1. Composition of the samples analysed in Figure S8, highlighting the volume fractions of CNCs (v_C) and ZIF-8 (v_Z), in place of the mass fraction values, and the resulting parameters of the rheology data fit with the Herschel-Bulkley model ($\boldsymbol{\sigma} = \boldsymbol{\sigma_y} + \boldsymbol{K\dot{\gamma}^n}$) or Power Law ($\boldsymbol{\sigma} = \boldsymbol{K\dot{\gamma}^n}$).

Sample	v_C [%]	v_Z [%]	σ_y [Pa]	K [Pa·s^n]	*n*
CNC $w_{5.19}$	3	0	-	1.38	0.42
$\alpha_{0.1}$ $w_{4.9}$	2.74	0.27	-	0.73	0.49
$\alpha_{0.2}$ $w_{4.7}$	2.50	0.50	-	0.21	0.60
α_1 $w_{3.9}$	1.50	1.50	-	0.046	0.70
$\alpha_5 w_{3.1}$	0.50	2.50	-	0.0029	0.94
α_{10} $w_{2.9}$	0.27	2.74	-	0.0019	0.98
ZIF-8 $w_{2.7}$	0	3	0.021	0.0028	0.91

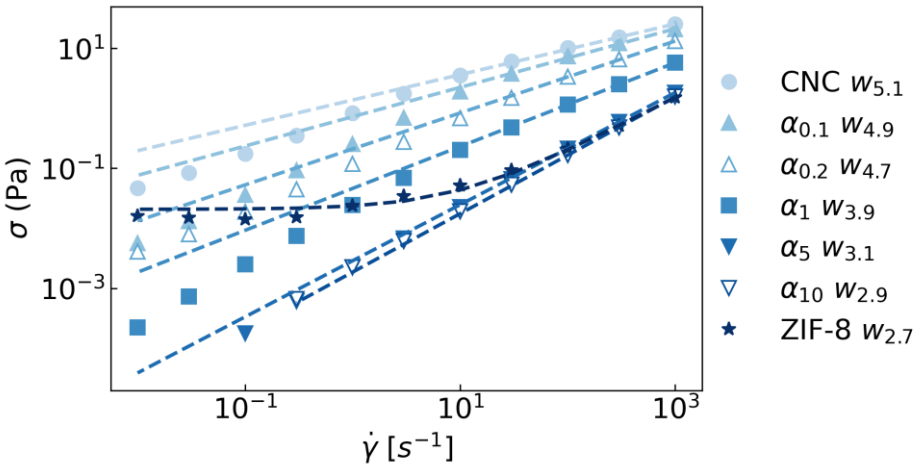

Figure S8. Stress vs. shear rate plots of CNC, ZIF-8, and mixed CNC:ZIF-8 suspensions at different α values. The dashed lines represent the Herschel-Bulkley fit (for ZIF-8) and Power Law fit.

The appearance of ZIF-8 and CNCs suspensions during shearing was investigated by rheo-optical methods by coupling a digital camera to the rheometer (Figure S9).

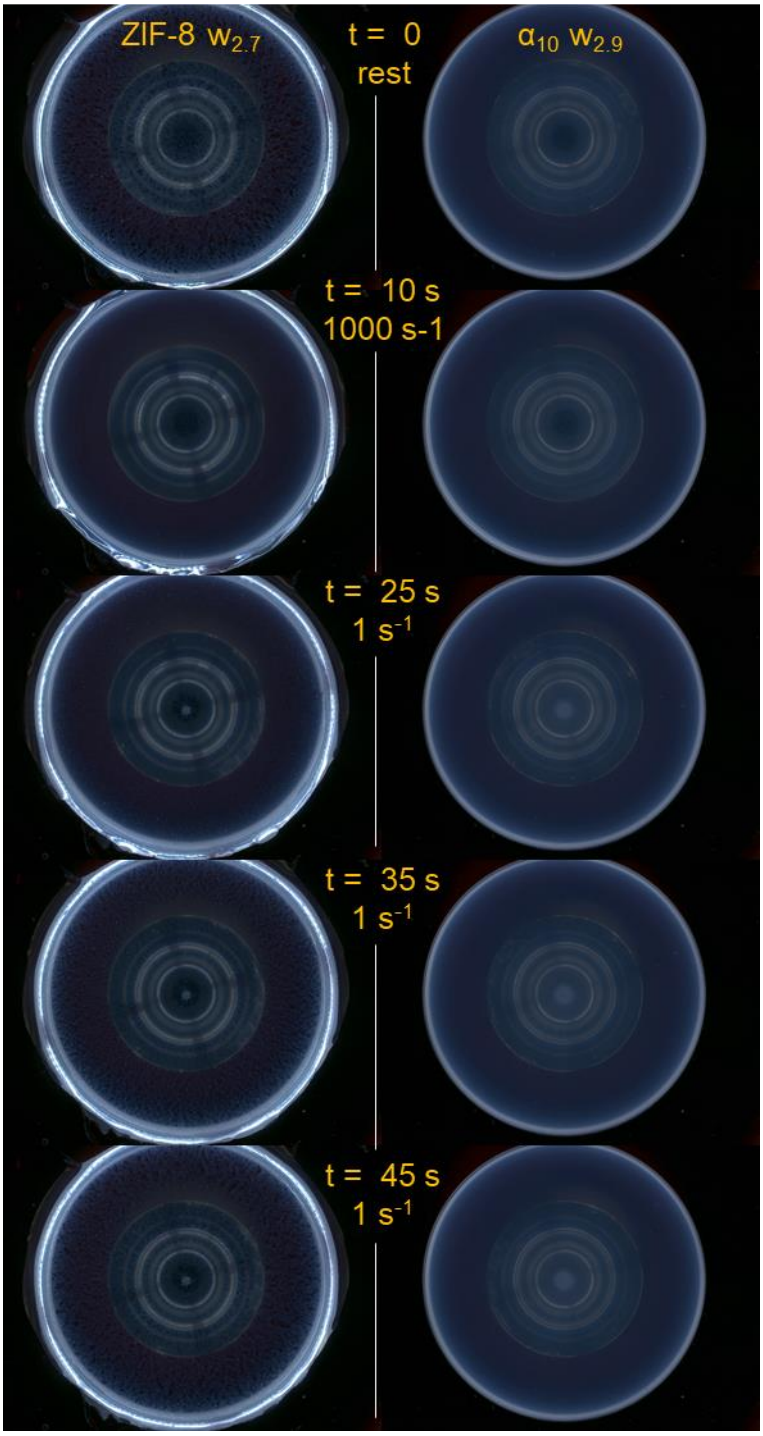

Figure S9. Rheo-optical images of sheared ZIF-8 $w_{2.7}$ suspension (left column) and α_{10} $w_{2.9}$ (right column) with the same volume fraction (φ=0.03). The shear values and duration are reported in the figure. It can be seen that the ZIF-8 suspension starts forming a percolated network between 25 and 35s, whereas sample α_{10} $w_{2.9}$ did not exhibit any change.

The azimuthally-averaged scattering intensity at a specific *q* value can be used to measure the increase of particles mass concentration during filtration (Pignon et al., 2012; Semeraro et al., 2020). In this work, the intensity at q=1 nm^{-1} was chosen, as the scattering intensity at this value was not affected by the variation of the structure factor S(q) with the samples' concentration. The evolution of I(q=1 nm^{-1}) during the filtration of a α_1 w_3 suspension is shown in Figure S10.

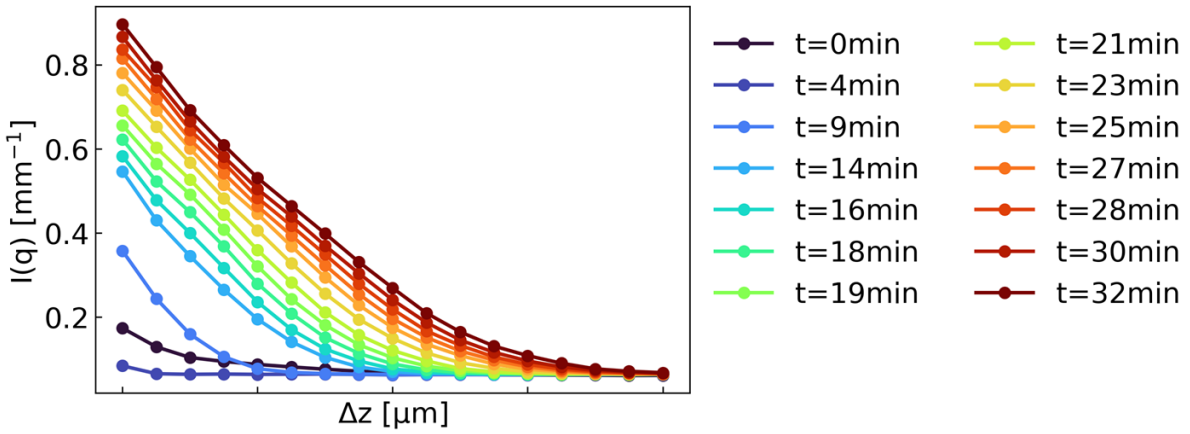

Figure S10. Evolution of the azimuthally-averaged scattering intensity at q = 1 nm^{-1} of a α_1 w_3 suspension during frontal filtration, measured in situ with SAXS.

Figure S11 shows the 2D scattering intensities collected during the *in situ* filtration of the sample α_1 w_3, as a function of time (y axis) and distance from the support membrane (x axis). These patterns were also used to compute the anisotropy level with the software *SASET* (Muthig et al., 2013).

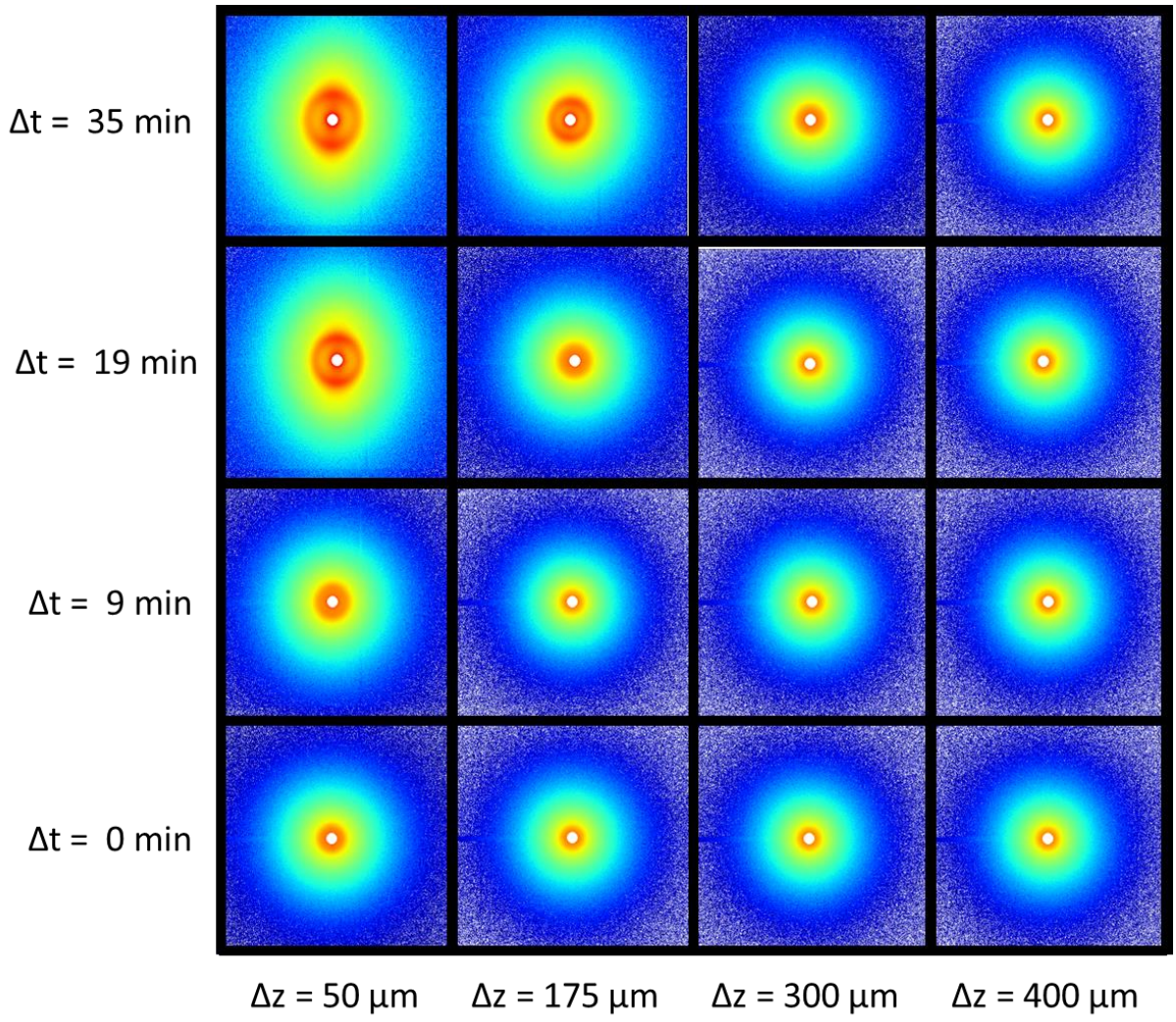

Figure S11. 2D scattering patterns acquired during the in situ SAXS filtration of a α_1 w_3 suspension, as a function of time (y axis) and distance from the membrane (x axis) distances.

The *ex situ* filtration deposit was prepared from a $\alpha_1 w_{1.4}$ suspension for 72 h and analysed later at TRUSAXS (ESRF, Grenoble) without removing the sample from the filtration cell. The suspension contained 0.92 wt. % CNCs and 0.48 wt. % ZIF-8 (Figure S12).

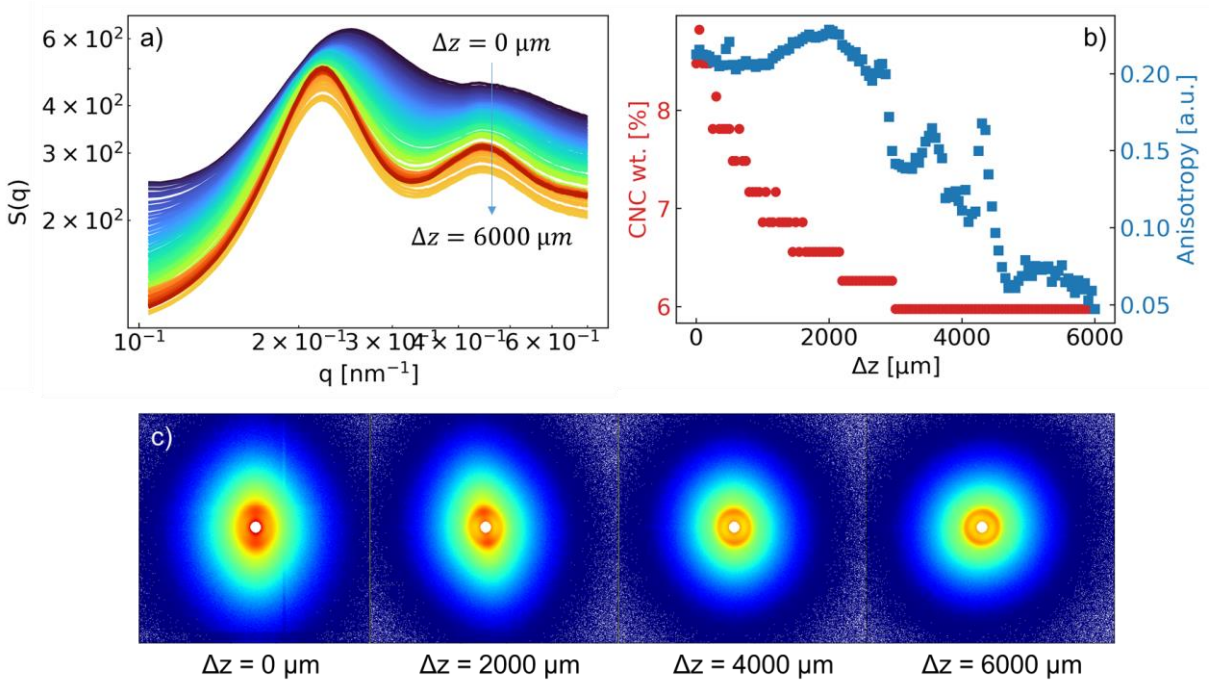

Figure S12. Structure factor S(q) the filtration deposit (a), calculated concentration of CNC from structure factor and scattering anisotropy (b), 2D scattering patterns at selected distances from the membrane (c).

Finally, thermogravimetric analysis (TGA) was performed to confirm the mass ratio between the CNCs and ZIF-8 in the filtration deposits (Figure S13).

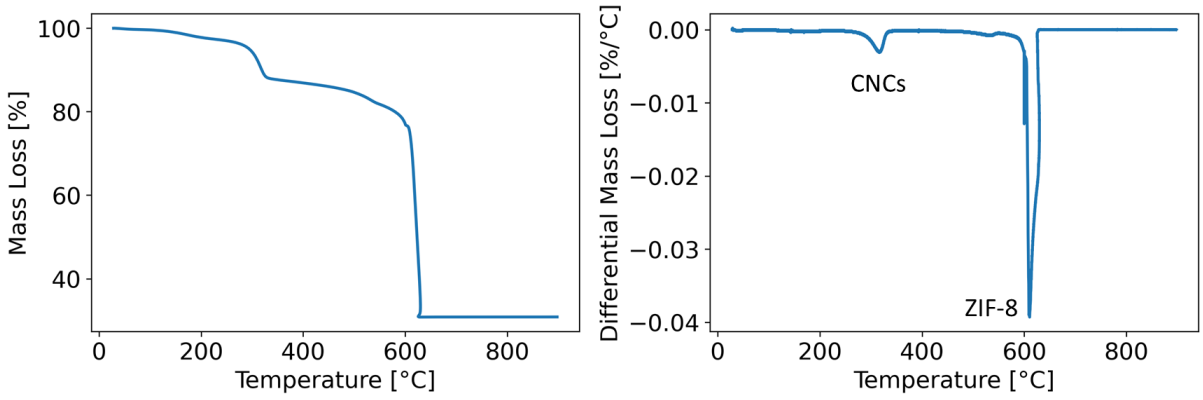

Figure S13. Thermogravimetric analysis of a α_{10} filtration dried deposit, obtained after 48h of frontal filtration. The differential mass loss curve (right) shows the peak belonging to the degradation of CNCs around 300°C, and a further peak at ca. 600°C, which relates to ZIF-8 degradation. The ratio between the area under the curve of the two integration peaks confirmed that the sample contained 1:10 CNC:ZIF-8 volume ratio.

Bibliography

Almasoudi, A., & Mokaya, R. (2012). Preparation and hydrogen storage capacity of templated and activated carbons nanocast from commercially available zeolitic imtablazolate framework. *J. Mater. Chem.*, *22*(1), 146–152. https://doi.org/10.1039/C1JM13314D

Muthig, M., Prévost, S., Orglmeister, R., & Gradzielski, M. (2013). *SASET*: A program for series analysis of small-angle scattering data. *Journal of Applied Crystallography*, *46*(4), 1187–1195. https://doi.org/10.1107/S0021889813016658

Pignon, F., Abyan, M., David, C., Magnin, A., & Sztucki, M. (2012). In Situ Characterization by SAXS of Concentration Polarization Layers during Cross-Flow Ultrafiltration of Laponite Dispersions. *Langmuir*, *28*(2), 1083–1094. https://doi.org/10.1021/la201492z

Semeraro, E. F., Hengl, N., Karrouch, M., Michot, L. J., Paineau, E., Jean, B., Putaux, J.-L., Lancelon-Pin, C., Sharpnack, L., & Pignon, F. (2020). Layered organization of anisometric cellulose nanocrystals and beidellite clay particles accumulated near the membrane surface during cross-flow ultrafiltration: In situ SAXS and ex situ SEM/WAXD characterization. *Colloids and Surfaces A: Physicochemical and Engineering Aspects*, *584*, 124030. https://doi.org/10.1016/j.colsurfa.2019.124030